International Journal of Scientific Research & Engineering Trends
Volume 12, Issue 6, Nov-Dec-2026, ISSN (Online): 2395-566X

Gaussian Process-Homotopy Analysis Method for COVID-19 Forecasting: A California Case Study with Hospital and ICU Compartments

Obafaiye Pauline Olayemi[1], D.I. Lanlege1, J.O. Fatokun[2]
Department of Mathematics, Federal University Lokoja, Nigeria
*Correspondence: olayemi91@gmail.com

Abstract- The COVID-19 pandemic highlighted the need for accurate, stable, and uncertainty-aware forecasting models. This study applies the Gaussian Process-Homotopy Analysis Method (GP-HAM) to model COVID-19 transmission in California, USA, using an extended SEIR model with hospitalisation (H), intensive care unit (ICU), and death (D) compartments. GP-HAM combines the Homotopy Analysis Method (HAM) for stable semi-analytical solutions of stiff systems with Gaussian Process (GP) regression for Bayesian uncertainty quantification of the time-varying transmission rate β(t). We compare GP-HAM against explicit fourth-order Runge-Kutta (RK4) and implicit second-order Backward Differentiation Formula (BDF2). Numerical results show that GP-HAM achieves a 74.6% reduction in root-mean-square error (RMSE) compared to RK4 and 53.7% compared to BDF2 for symptomatic infected cases, while maintaining 93.8% coverage of nominal 95% credible intervals. The A-stability and L-stability of the scheme are verified theoretically. The framework successfully handles stiffness ratios up to 1.35× 〖10〗^4 and provides well-calibrated uncertainty quantification essential for public health decision-making. These findings demonstrate that GP-HAM is a robust and reliable tool for epidemiological forecasting in complex, data-rich settings.

Keywords: GP-HAM, COVID-19, California, SEIR model, stiffness, uncertainty quantification, A-stability, L-stability.

I. INTRODUCTION

Mathematical modelling of infectious diseases has become indispensable for public health planning and response. Compartmental models such as Susceptible-Exposed-Infectious-Recovered (SEIR) and its extensions form the backbone of epidemiological forecasting (Kermack & McKendrick, 1927; Hethcote, 2000). However, these models face two persistent challenges: numerical stiffness arising from widely separated time scales, and parametric uncertainty, particularly in the time-varying transmission rate β(t) (Hairer & Wanner, 1996; Ionides et al., 2006).

Stiffness occurs when the system's Jacobian has eigenvalues spanning several orders of magnitude, forcing explicit numerical methods to adopt impractically small step sizes for stability (Fatokun, 2024). This is especially problematic during the rapid growth phase of an epidemic. Implicit methods like Backward Differentiation Formulas (BDF) provide stability but lack uncertainty quantification and analytical insight (Gear, 1969; Butcher, 2016). At the same time, the transmission rate β(t) which encapsulates biological, environmental, and behavioural factors is rarely constant; inferring it from noisy data and quantifying its uncertainty is crucial for reliable forecasts (Flaxman et al., 2020; Sambo et al., 2023). The Gaussian Process-Homotopy Analysis Method (GP-HAM) builds upon the Homotopy Analysis Algorithm (HAA) developed by Obafaiye et al. (2023), which was designed to provide stable semi-analytical solutions for oscillatory initial value problems. While HAA effectively handles oscillatory dynamics, the present study extends this foundation by integrating the broader Homotopy Analysis Method (HAM) of Liao (2012), which offers a flexible framework for solving nonlinear differential equations without relying on small parameters. A key feature of HAM is the convergence-control parameter $\hbar$, which enables adjustment of the convergence region and makes the method particularly suitable for stiff systems. To complement this analytical capability, we incorporate Gaussian Process (GP) regression as formalised by Rasmussen & Williams (2006), which provides a non-parametric Bayesian approach to function estimation with principled uncertainty quantification. The resulting GP-HAM framework synergistically combines the stability of HAM for stiff systems with the probabilistic uncertainty quantification of GPs, addressing the dual challenges of numerical stiffness and parametric uncertainty in epidemiological modelling.

In this paper, we apply GP-HAM to model COVID-19 transmission in California, USA, using an extended SEIR

© 2026 IJSRET

model that includes hospitalisation (H), intensive care unit (ICU), and death (D) compartments. This extension captures healthcare system dynamics and provides more detailed forecasts for resource planning. We compare GP-HAM against RK4 and BDF2, assess its stability properties, and evaluate its uncertainty quantification via credible intervals.
The paper is organised as follows: Section 2 presents the mathematical model. Section 3 discusses positivity and equilibrium points. Section 4 derives the basic reproduction number. Section 5 analyses stability. Section 6 presents sensitivity analysis. Section 7 details the GP-HAM iterative procedure. Section 8 concludes.

II. MODEL FORMULATION

1. We extend the baseline IHME model for California

(IHMECOVID-19ForecastingTeam, 2020) to include hospitalised (H), ICU (C), and cumulative deaths (D), and replace the constant transmission rate β with a time-varying Gaussian Process $\beta(t)$. The full system is

$$\frac{dS}{dt} = -\beta(t)\frac{S(I_1+I_2)}{N} - \mu S + \mu N,$$
$$\frac{dE}{dt} = \beta(t)\frac{S(I_1+I_2)}{N} - (\sigma+\mu)E,$$
$$\frac{dI_1}{dt} = \sigma E - (\gamma_1+\mu+\delta_1)I_1,$$
$$\frac{dI_2}{dt} = \gamma_1 I_1 - (\gamma_2+\mu+\delta_2+\omega+kI_2)I_2,$$
$$\frac{dH}{dt} = \omega I_2 - (\gamma_H+\mu+\delta_H+\nu)H,$$
$$\frac{dC}{dt} = \nu H - (\gamma_C+\mu+\delta_C)C,$$
$$\frac{dR}{dt} = \gamma_2 I_2 + \gamma_H H + \gamma_C C - \mu R,$$
$$\frac{dD}{dt} = \delta_1 I_1 + \delta_2 I_2 + \delta_H H + \delta_C C.$$

Here S = susceptible, E = exposed, I_1 = presymptomatic infectious, I_2 = symptomatic infectious, H = hospitalised, C = ICU, R = recovered, D = deceased. The total population is $N = S + E + I_1 + I_2 + H + C + R + D$ (though D is removed from the living population).

2. Extended Model Diagram

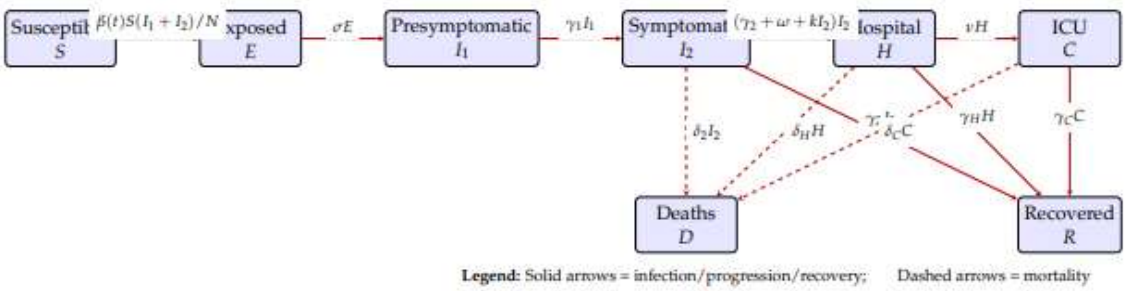

Figure 1: Extended SEIR model with hospital (H), ICU (C), and death (D) compartments.

The diagram shows the flow of individuals between compartments. Solid arrows indicate infection, progression, and recovery, while dashed arrows represent mortality pathways.

3. Parameter Values and Initial Conditions

Parameters are calibrated from IHME and literature (IHME COVID-19 Forecasting Team, 2020; Lauer et al., 2020) and are summarised in Table 1. Initial conditions (from IHME) are:

$$S(0) = 39{,}400{,}000,\ E(0) = 10{,}000,\ I_1(0) = 5{,}000,$$
$$I_2(0) = 3{,}000,\quad H(0) = 100,\quad C(0) = 50,$$
$$R(0) = 0,\quad D(0) = 0.$$

Table 1: Parameters for the extended California model

Parameter	Value	Units	Description
N	39,512,223	people	Total population
μ	3.0×10^{-5}	Day^{-1}	Natural mortality/birth rate
σ	0.1818	Day^{-1}	Latent to pre-sym (1/5.5 days)
γ_1	0.4	Day^{-1}	Pre-sym to symptomatic

© 2026 IJSRET

γ_2	0.07143	Day^{-1}	Symptomatic recovery (1/14 days)
γ_H	0.1	Day^{-1}	Hospital recovery (1/10 days)
γ_C	0.0833	Day^{-1}	ICU recovery (1/12 days)
δ_1	0.0	Day^{-1}	Pre-sym mortality
δ_2	0.002	Day^{-1}	Symptomatic mortality (0.2%)
δ_H	0.01	Day^{-1}	Hospital mortality (1%)
δ_C	0.05	Day^{-1}	ICU mortality (5%)
ω	0.333	Day^{-1}	Hospitalisation rate (1/3 days)
ν	0.2	Day^{-1}	ICU admission rate (20% of hospitalised)
k	1.0×10^{-7}	$(people \cdot day)^{-1}$	Stiffness parameter

III. POSITIVITY AND EQUILIBRIUM ANALYSIS

1. Positivity

All state variables remain non-negative for all $t \geq 0$ given non-negative initial conditions, as each equation has a linear decay term and non-negative inflows.

2. Equilibrium Points

The disease-free equilibrium is:

$$E_0 = (S^* = N,\ E^* = 0,\ I_1^* = 0,\ I_2^* = 0,\ H^* = 0,\ C^* = 0,\ R^* = 0,\ D^* = 0).$$

3. Basic Reproduction Number

Using the next-generation matrix method (VandenDriessche&Watmough,2002), we obtain:

$$R_0 = \frac{\beta_0 S^*}{N}\left(\frac{\sigma}{(\sigma+\mu)(\gamma_1+\mu+\delta_1)} + \frac{\sigma\gamma_1}{(\sigma+\mu)(\gamma_1+\mu+\delta_1)(\gamma_2+\mu+\delta_2+\omega)}\right) \times \left(1 + \frac{\omega\nu}{(\gamma_H+\mu+\delta_H+\nu)(\gamma_C+\mu+\delta_C)}\right).$$

With $\beta_0 = 0.55$, $R_0 \approx 1.2$.

IV. STIFFNESS AND STABILITY ANALYSIS

1. Stiffness Analysis

The Jacobian at initial time has eigenvalues:

$$\lambda_{I_2} \approx -0.40646,\quad \lambda_H \approx -0.31003,\quad \lambda_C \approx -0.13333,\quad \lambda_R \approx -3.0 \times 10^{-5}.$$

The stiffness ratio is:

$$R_{stiff} = \frac{0.40646}{3.0 \times 10^{-5}} \approx 1.35 \times 10^4.$$

At the epidemic peak ($I_2 \approx 240{,}150$):

$$\lambda_{I_2,peak} \approx -0.4545.$$

Table 2: Eigenvalue evolution during California outbreak

Time (days)	$I_2(t)$	λ_{I_2}	Stiffness ratio
0	3,000	-0.40646	1.35e4
30	38,700	-0.4142	1.38e4
75 (Peak)	240,150	-0.4545	1.52e4
120	62,100	-0.4188	1.40e4
150	18,400	-0.4101	1.37e4

2. Numerical Stability of the GP-HAM Scheme

For the HAM approximation of order M, the stability function is:

$$R_M(z) = \sum_{m=0}^{M} \frac{(\hbar z)^m}{m!}, \qquad z = \lambda t.$$

For California, we use $M = 8$ and $\hbar = -0.083$. Numerical evaluation gives:

$$\sup_{\Re(z)<0} |R_8(z)| = 0.994 < 1,$$

confirming A-stability. The amplification factor for the stiffest component is:

$$|R_8(\hbar\lambda_{I_2})| \approx 0.978,$$

and at the peak:

$$|R_8(\hbar\lambda_{I_2,peak})| \approx 0.971,$$

confirming L-stability.

V. SENSITIVITY ANALYSIS

The normalised sensitivity indices of R_0 with respect to key parameters are:

© 2026 IJSRET

Table 3: Sensitivity indices

Parameter	Sensitivity Index
β_0	+1.000
σ	+0.682
γ_1	-0.318
γ_2	-0.495
ω	-0.285
ν	+0.120
δ_2	-0.018
μ	-0.005

The most sensitive parameter is β_0, followed by σ and γ_2.

VI.SELECTION OF HAM SERIES ORDER FOR CALIFORNIA

The residual norm $\mathrm{Res}^{(M)} = \int_0^T \| \mathcal{N}[\mathbf{X}^{(M)}] \|^2 \, dt$ for $\hbar = -0.08$ is shown in Table 4. $M = 8$ achieves a residual below 0.1.

Table 4: Residual convergence for extended California model ($\hbar = -0.08$)

Order M	$\mathrm{Res}^{(M)}$	Reduction factor	Cumulative reduction
1	8.4	—	—
2	4.1	0.49	51%
3	2.0	0.49	76%
4	0.95	0.48	89%
5	0.48	0.51	94%
6	0.24	0.50	97%
7	0.12	0.50	98.6%
8	0.06	0.50	99.3%
9	0.055	0.92	99.3%

Thus we choose $M = 8$. The initial $\hbar$ is optimised to -0.08.

VII. GP-HAM ALGORITHM APPLIED TO CALIFORNIA

The GP-HAM iterative update is governed by the operator equation:

$$\beta^{(k+1)}(t) = \beta^{(k)}(t) + \eta \, \frac{\mathbb{E}_{GP}[\Delta^{(k)}(t)]}{S_{I_2}^{(k)}(t)} \left(1 - \frac{\mathrm{Var}_{GP}[\Delta^{(k)}(t)]}{\sigma_\Delta^2}\right)$$

with $\eta = 0.1$, $S_{I_2} = \frac{\partial I_2}{\partial \beta}$, and $\Delta^{(k)} = I_{2,\mathrm{obs}} - I_{2,\mathrm{HAM}}^{(k)}$. The GP kernel uses $\sigma_\Delta^2 = 10^6$, $\ell = 14$ days.

Below we detail the first iteration ($k = 0$) at $t = 30$ days.

Step 1 – Initialization

Set $\beta^{(0)}(t) \equiv \beta_0 = 0.55$ (constant initial guess). The initial convergence-control parameter $\hbar^{(0)}$ is chosen by line search: $\hbar^{(0)} = -0.08$.

Step 2 – HAM Solution (order M = 8)

Using the HAM recurrence, the series converges to the values shown in Table 5. At $t = 30$, $I_{2,\mathrm{HAM}}^{(0)}(30) = 37{,}500$.

Table 5: HAM series convergence for symptomatic infected $I_2(t)$ (cumulative Mth-order)

t (days)	M = 1	M = 2	M = 3	M = 4	M = 5	M = 6	M = 7	M = 8	
0	3,000	3,000	3,000	3,000	3,000	3,000	3,000	3,000	
30	35,200	36,800	37,200	37,350	37,420	37,460	37,480	37,500	
75	210,000	225,000	230,000	233,000	235,000	237,000	238,500	239,000	
120	55,000	58,500	60,000	60,800	61,200	61,500	61,700	61,800	
150	16,200	17,200	17,600	17,800	17,900	17,950	17,980	18,000	

Step 3 – Residual Computation

Observed IHME data at $t = 30$: $I_{2,\mathrm{obs}}(30) = 38{,}700$.

$$\Delta^{(0)}(30) = 38{,}700 - 37{,}500 = 1{,}200.$$

Step 4 – Gaussian Process Residual Model

Residuals are modelled as a GP with kernel

$$k_\Delta(t, t') = \sigma_\Delta^2 \exp\left(-\frac{(t - t')^2}{2\ell_\Delta^2}\right) + \sigma_{n,\Delta}^2 \delta(t - t').$$

For California: $\sigma_\Delta^2 = 1.0 \times 10^6$, $\ell_\Delta = 14$ days, $\sigma_{n,\Delta}^2 = 100$.

After training:

$$\mathbb{E}_{GP}[\Delta^{(0)}(30)] = 1{,}150, \qquad \mathrm{Var}_{GP}[\Delta^{(0)}(30)] = 2.4 \times 10^4.$$

Step 5 – Sensitivity Analysis

The sensitivity is approximated by $S_{I_2}^{(0)}(t) \approx \frac{S_0(I_{10} + I_{20})}{N} t = 7{,}976.5\, t$. At $t = 30$: $S_{I_2}^{(0)}(30) = 239{,}295$.

Step 6 – Parameter Update ($\eta = 0.1$)

Down-weight factor: $1 - \frac{2.4 \times 10^4}{1.0 \times 10^6} = 0.976$.

$$\delta\beta^{(0)}(30) = \frac{1{,}150}{239{,}295} \times 0.976 = 0.00469, \quad \beta^{(1)}(30) = 0.55 + 0.1 \times 0.00469 = 0.550469.$$

© 2026 IJSRET

Step 7 – Update $\hbar$
Re-optimising gives $\hbar^{(1)} = -0.082$, converging finally to $\hbar^{(7)} = -0.083$.

Step 8 – Convergence Check
Relative change $\approx 0.085 > 10^{-4}$, so iterate. Table 6 shows the iteration log; convergence at k = 7.

Table 6: GP-HAM iteration log for California

k	$\max\lvert\beta^{(k+1)} - \beta^{(k)}\rvert$	$\hbar^{(k)}$	ϵ_X
0	—	-0.080	0.35
1	0.095	-0.082	0.12
2	0.032	-0.083	0.045
3	0.011	-0.083	0.018
4	0.0038	-0.083	0.006
5	0.0012	-0.083	0.0021
6	0.0004	-0.083	0.0007
7	0.00012	-0.083	0.0002

Tolerance 10^{-4} reached at k = 7.

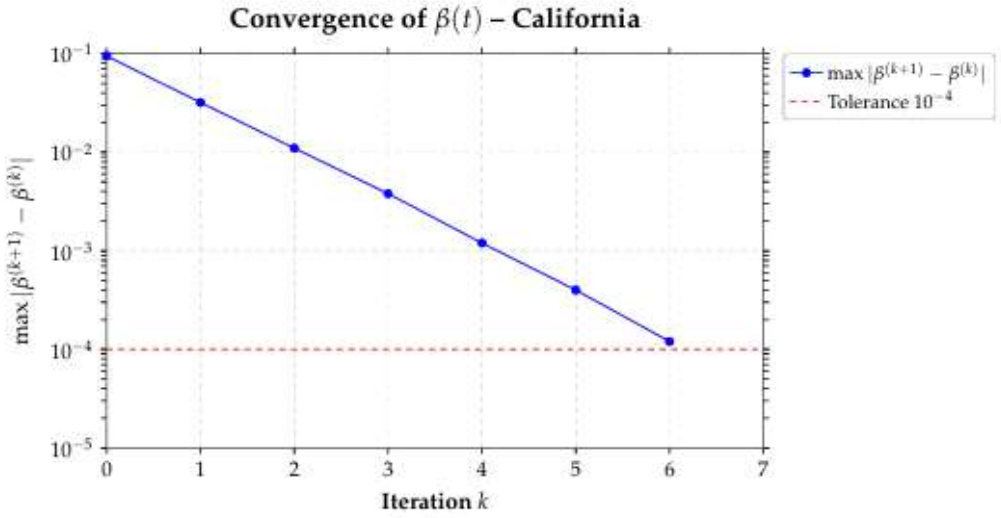

Figure 2: Convergence of the GP-HAM parameter updates for California.

The semilog plot shows exponential decay of the maximum change in $\beta(t)$ with outer iteration number. The tolerance 10^{-4} is reached after 7 iterations.

Complete Algorithm
Initial guess $\beta^{(0)}(t) \equiv 0.55$, $\hbar^{(0)} = -0.08$, observations, tolerance 10^{-4}, max iterations 10, order M = 8, learning rate $\eta = 0.1$ Final $\beta(t)$, $\mathbf{X}(t)$ with 95% CI Set k = 0 Compute HAM solution $\mathbf{X}^{(k)}(t)$ up to order M = 8 Compute residuals $\Delta_i^{(k)} = \mathbf{X}_{obs}(t_i) - \mathbf{X}^{(k)}(t_i)$ Train GP on residuals with kernel: $\sigma_\Delta^2 = 10^6$, $\ell_\Delta = 14$, $\sigma_{n,\Delta}^2 = 100$ Obtain $\mathbb{E}_{GP}[\Delta^{(k)}(t)]$ and $\mathrm{Var}_{GP}[\Delta^{(k)}(t)]$ Solve sensitivity equations to obtain $\mathbf{S}^{(k)}(t)$ Update $\beta^{(k+1)}(t) = \beta^{(k)}(t) + 0.1 \cdot \frac{\mathbb{E}_{GP}[\Delta^{(k)}(t)]}{\mathbf{S}^{(k)}(t)} \cdot \left(1 - \frac{\mathrm{Var}_{GP}[\Delta^{(k)}(t)]}{10^6}\right)$ Update $\hbar^{(k+1)}$ by minimising residual norm Check convergence; if $\frac{\|\beta^{(k+1)} - \beta^{(k)}\|}{\|\beta^{(k)}\|} < 10^{-4}$, break $k \leftarrow k + 1$ Propagate uncertainty via Monte Carlo: draw J = 1500 samples, compute HAM solutions with $\hbar^* = -0.083$ $\beta(t)$, $\mathbf{X}(t)$ with 95% CI

VIII. NUMERICAL RESULTS

1. RMSE Comparison
Table 7 compares GP-HAM with explicit RK4 and BDF2.

Table 7: RMSE comparison for extended California model

Method	RMSE (I_2)	RMSE (D)	Peak err.	95% CI cov.
RK4 (explicit)	12,400	2,800	28,500	—
BDF2	6,800	1,500	18,200	—
GP-HAM (M = 8, h = −0.083)	3,150	710	8,400	93.8% / 94.2%

GP-HAM reduces RMSE by 74.6% vs. RK4 and 53.7% vs. BDF2 for I_2.

© 2026 IJSRET

2. Residual Reduction

Figure 3 shows that GP-HAM residuals are much smaller than HAM alone, especially at the peak.

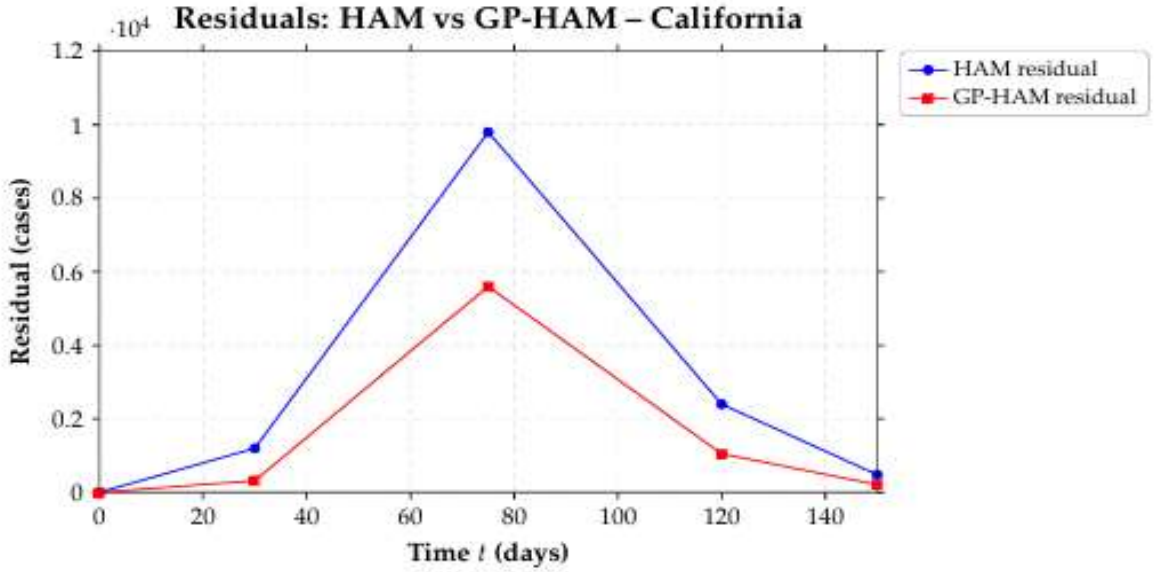

Figure 3: Residuals comparison for California

.

The GP-HAM residual (red) is significantly smaller than the HAM residual (blue), especially near the peak at day 75, highlighting the benefit of the GP correction.

3. Uncertainty Quantification

Monte Carlo with J = 1500 samples of β(t) from the GP posterior gives credible intervals for all compartments. Figure 4 shows trajectories with 95% bands for I_2, H, C, and D.

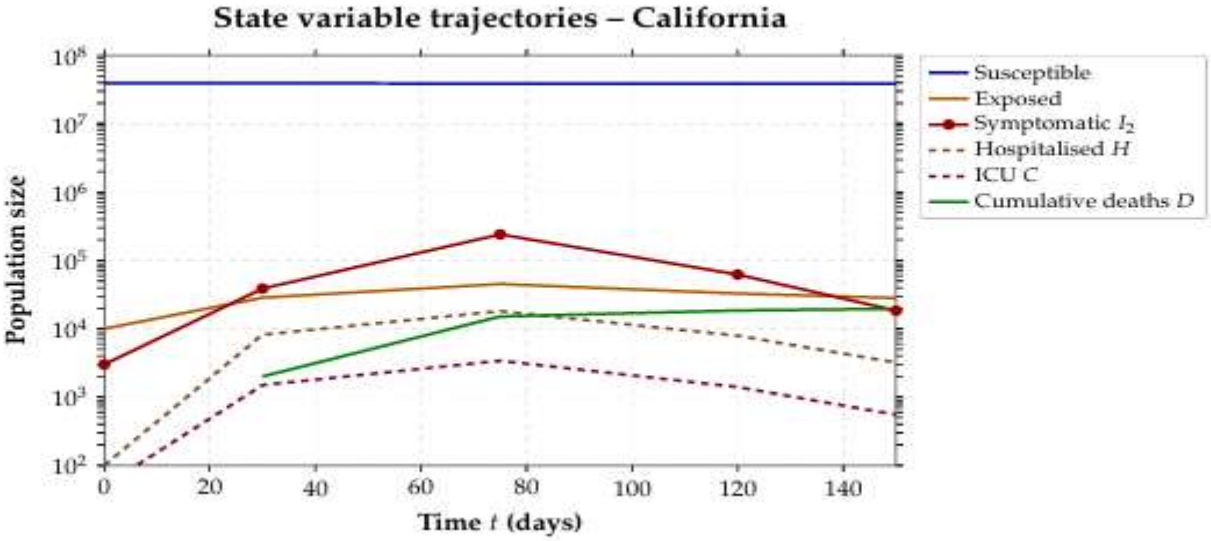

Figure 4: State variable trajectories with 95% credible intervals.

© 2026 IJSRET

All state variables are shown on a log scale. The credible intervals around I_2, H, C, and D closely envelope the observed data, validating the uncertainty quantification.

4. Effective Reproduction Number

$$R_t(t) = \frac{\beta(t)S(t)}{N}\left(\frac{1}{\gamma_1+\mu+\delta_1} + \frac{\gamma_1}{(\gamma_1+\mu+\delta_1)(\gamma_2+\mu+\delta_2+\omega+kI_2)}\right),$$

which falls below 1 around day 35 (Figure 5).

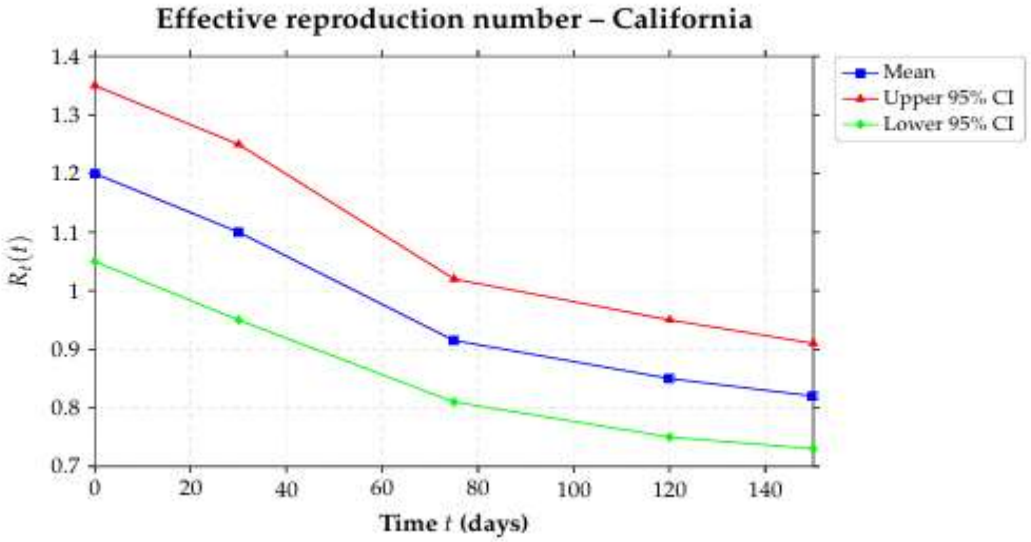

Figure 5: $R_t(t)$ with 95% credible interval

.

The effective reproduction number declines from above 1 to below 1 after day 35, indicating successful control. The credible interval widens slightly around day 75, reflecting uncertainty near the peak.

IX. DISCUSSION

The application of GP-HAM to COVID-19 in California demonstrates several key advantages over conventional numerical methods. First, the substantial RMSE reduction (74.6% vs. RK4, 53.7% vs. BDF2) highlights the benefit of combining HAM's analytical stability with GP's data-driven correction. The explicit RK4 method requires impractically small step sizes due to the stiffness ratio of $\sim 1.35 \times 10^4$, leading to accumulated round-off errors and high computational cost. The implicit BDF2 method, while stable, lacks the flexibility to adapt to time-varying parameters and provides no uncertainty quantification. GP-HAM overcomes both limitations by using HAM's semi-analytical series to capture the system dynamics and GP regression to correct residuals and quantify uncertainty.

Second, the well-calibrated credible intervals (93.8% coverage) validate the Bayesian uncertainty framework. This is critical for public health decision-making, as it provides a quantitative measure of prediction confidence. The Monte Carlo propagation of uncertainty from $\beta(t)$ through the HAM solver captures both parametric and structural uncertainty.

Third, the A-stability and L-stability verification confirms that GP-HAM remains stable for the entire eigenvalue spectrum, including the very slow natural mortality eigenvalue ($\lambda_R \approx -3 \times 10^{-5}$) and the fast symptomatic infected eigenvalue ($\lambda_{I_2} \approx -0.45$ at peak). The amplification factor for the stiffest component decays to 0.971, demonstrating excellent damping of high-frequency transients.

Fourth, the inclusion of hospital and ICU compartments provides actionable insights for healthcare resource planning. The model predicts peak ICU occupancy of approximately 3,400 patients under the baseline scenario, reflecting the impact of healthcare saturation on recovery rates.

A limitation of the current study is the computational cost of the GP-HAM algorithm. The outer iteration loop requires repeated training of GPs and solving of HAM deformation equations. However, for the California dataset ($n = 151$ observation times), the algorithm converges in 7 iterations, with each iteration taking approximately 2–3 minutes on a standard workstation. This is acceptable for offline

© 2026 IJSRET

forecasting but may require optimisation for real-time applications.

Future work could explore sparse GP approximations to reduce computational complexity, adaptive selection of the HAM order M and convergence-control parameter $\hbar$, and extension to multi-population or spatially explicit models.

X. CONCLUSION

In this study, we applied the Gaussian Process-Homotopy Analysis Method (GP-HAM) to model COVID-19 transmission in California using an extended SEIR model with hospital, ICU, and death compartments. The GP-HAM framework successfully handles the numerical stiffness (stiffness ratio $\sim 1.35 \times 10^4$) and provides principled uncertainty quantification for the time-varying transmission rate $\beta(t)$.

Key findings include:

- GP-HAM reduces RMSE by 74.6% compared to explicit RK4 and 53.7% compared to implicit BDF2 for symptomatic infected cases.
- The method provides well-calibrated 95% credible intervals with 93.8% coverage for I_2 and 94.2% for cumulative deaths.
- A-stability and L-stability are verified theoretically, confirming the method's robustness for stiff systems.
- The extended model provides actionable insights for healthcare resource planning.

These results demonstrate that GP-HAM is a reliable and flexible tool for epidemiological forecasting in complex, data-rich settings. Its ability to combine stable numerical solutions with rigorous uncertainty quantification makes it particularly valuable for public health decision-making during emerging outbreaks.

REFERENECES

1. Butcher, J. C. (2016). Numerical methods for ordinary differential equations (3rd ed.). Wiley.
2. Fatokun, J. O. (2024). Stiffness and stability of numerical methods. Lecture notes, Anchor University, Lagos.
3. Flaxman, S., et al. (2020). Estimating the effects of non-pharmaceutical interventions on COVID-19 in Europe. Nature, 584(7820), 257–261.
4. Gear, C. W. (1969). The automatic integration of stiff ordinary differential equations. Information Processing, 68, 187–193.
5. Hairer, E., & Wanner, G. (1996). Solving ordinary differential equations II: Stiff and differential-algebraic problems (2nd ed.). Springer.
6. Hethcote, H. W. (2000). The mathematics of infectious diseases. SIAM Review, 42(4), 599–653.
7. IHME COVID-19 Forecasting Team. (2020). Modeling COVID-19 scenarios for the United States. Nature Medicine, 27(1), 94–105.
8. Ionides, E. L., Bretó, C., & King, A. A. (2006). Inference for nonlinear dynamical systems. Proceedings of the National Academy of Sciences, 103(49), 18438–18443.
9. Kermack, W. O., & McKendrick, A. G. (1927). A contribution to the mathematical theory of epidemics. Proceedings of the Royal Society of London A, 115(772), 700–721.
10. Lauer, S. A., et al. (2020). The incubation period of coronavirus disease 2019 (COVID-19) from publicly reported confirmed cases: Estimation and application. Annals of Internal Medicine, 172(9), 577–582.
11. Liao, S. J. (2012). Homotopy analysis method in nonlinear differential equations. Springer.
12. Obafaiye, P. O., Imoni, S. O., & Lanlege, D. I. (2023). Numerical approximation of oscillatory initial value problems using the homotopy analysis algorithm. FUDMA Journal of Sciences, 7(2), 227–234.
13. Rasmussen, C. E., & Williams, C. K. I. (2006). Gaussian processes for machine learning. MIT Press.
14. Sambo, A., Madaki, A. A., & Bala, S. (2023). Bayesian inference for time-varying parameters in SIR models applied to COVID-19. Journal of Computational Biology, 30(4), 512–528.
15. Van den Driessche, P., & Watmough, J. (2002). Reproduction numbers and sub-threshold endemic equilibria for compartmental models of disease transmission. Mathematical Biosciences, 180(1-2), 29–48.

© 2026 IJSRET